SOURCES, CONTROL, AND EFFECTS OF NOISE FROM AIRCRAFT PROPELLERS AND ROTORS

John S. Mixson, George C. Greene, and Thomas K. Dempsey

SUMMARY

Control of noise generated by aircraft propellers and rotors is important to minimize annoyance or discomfort felt by community residents and aircraft passengers. This paper describes recent NASA and NASA-sponsored research on the prediction and control of propeller and rotor source noise, on the analysis and design of fuselage-sidewall noise control treatments, and on the measurement and quantification of the response of passengers to aircraft noise. Source noise predictions are compared with measurements for conventional low-speed propellers, for new high-speed propellers (propfans), and for a helicopter. Results from a light aircraft demonstration program are described, indicating that about 5-dB reduction of flyover noise can be obtained without significant performance penalty. Sidewall design studies are described for interior noise control in light general aviation aircraft and in large transports using propfan propulsion. The weight of the added acoustic treatment is estimated and tradeoffs between weight and noise reduction are discussed. A laboratory study of passenger response to combined broadband and tonal propeller-like noise is described. Subject discomfort ratings of combined tone-broadband noises are compared with ratings of broadband (boundary layer) noise alone, and the relative importance of the propeller tones is examined.

INTRODUCTION

Noise generated by aircraft propellers and rotors can propagate into the airport community and into the aircraft interior causing annoyance and discomfort of residents and passengers. The importance of control is indicated by the large number of general aviation aircraft, the increasing use of fixed-wing and rotary-wing business aircraft, and the increasing number of propeller-driven commuter aircraft. In addition, the need to reduce fuel consumption has lead to the study of high-speed, large capacity, propeller-driven aircraft to be used in scheduled airline service as alternates to current jet aircraft. While developing noise control methods, it is also important to minimize the impact of noise control on the aircraft performance and weight.

Control of the noise at the source can be expected to reduce the impact on both community and passengers. This paper describes recent studies of the prediction and control of source noise generated by conventional low-speed propellers, by new high-speed propellers (propfans), and by helicopter rotors. In addition to source noise reduction, noise control treatment is usually required in the aircraft sidewall to provide a comfortable environment for passengers. Recent studies of the analysis and design of acoustic treatment for aircraft sidewalls are described for application to light general aviation aircraft and to large transports using propfan propulsion. Approaches to minimizing the added weight are also discussed. Minimizing the aircraft weight or performance penalty while providing an acceptable environment requires a detailed understanding of the responses of people to the noise. Therefore, the final topic discussed in this paper is the measurement of passenger response to noise and vibration environments, including a recent laboratory study using combined broadband noise and tonal propeller-type noise. The paper summarizes the objectives, recent results, and future trends of NASA and NASA-sponsored research in the three areas, with specific attention to applications to general aviation aircraft, helicopters, and advanced high-speed turboprop aircraft.

PROPELLER AND ROTOR NOISE PREDICTION

The purpose of NASA's propeller and helicopter-rotor noise research program is to provide a technology base for reducing noise with a minimum of performance, weight, and economic penalties. Noise prediction technology represents the most basic part of the program. The emphasis of this activity is on the understanding and prediction of noise using basic principles of physics. This requires a knowledge of the geometry, operating conditions, and aerodynamic characteristics of the propeller/rotor.

Low-Speed Propellers

Examples of noise calculations for low-speed propellers using recently developed technology (refs. 1-3) are shown in figures 1 and 2. Figure 1 shows a comparison of measured and calculated noise for a light, twin-engine transport aircraft. The data, obtained during an extensive flight test program (ref. 1), were taken at a propeller-tip Mach number of approximately 0.85, at an airspeed of approximately 55 m/s, and with one engine shutdown. The acoustic measurements were made in the plane of the propeller with a microphone mounted on a boom on the aircraft wing. The noise calculations were made using the two methods described in reference 3, both giving the same numerical results. The good agreement shown is typical of the comparisons over a range of flight conditions.

Figure 2 shows another comparison of measured and calculated results for low-speed propellers (ref. 2). The measurements were made during the evaluation of quiet propeller designs in an anechoic wind tunnel, as shown in the schematic on the right side of the figure. The data are for a 1/4-scale model of a light, single-engine aircraft propeller at an airspeed of approximately 30 m/s. Noise data were measured with a microphone mounted in the airstream 1 diameter from the center of propeller rotation. The acoustic pressure time history is presented for approximately two revolutions of the propeller. The almost perfect agreement is a result of very careful acoustic measurements and accurate calculations of the propeller aerodynamic characteristics.

High-Speed Propellers

High-speed propeller/rotor noise prediction technology is evolving rapidly (refs. 3-7). It is a difficult problem because of the relatively high tip Mach numbers, advanced blade geometry, and complex aerodynamic flow field. In addition, there is little acoustic data available to evaluate the predictions because there are no high-speed acoustic facilities for testing propellers.

A comparison of predicted and measured noise for a compromise test condition (ref. 8) is shown in figure 3. These results are for a 0.61-m diameter, two-bladed version of the high-speed propeller shown in the photograph. This propeller was designed for a freestream Mach number of 0.8 and was tested in an open-jet wind tunnel at a freestream Mach number of 0.3 with the propeller rpm increased so that the tip Mach number was equal to the design value of approximately 1.13. The noise measurements were made in an anechoic chamber surrounding the free jet with corrections applied for the shear-layer effects. The noise calculations were made using the method of reference 9, which includes only the effects of blade thickness and loading. The agreement for the lower harmonics is good; however, there is a tendency to underpredict the level of the fundamental.

This tendency to underpredict the fundamental is different from results (ref. 10) obtained in a hard-wall wind tunnel at freestream Mach numbers between 0.6 and 0.85. Reference 10 indicates that the noise level at the fundamental frequency is nearly constant for tip Mach numbers above 1.07. At a tip Mach number of 1.14, the noise level predicted by the method of reference 9 is 5 to 10 dB higher than the values measured in the hard-wall tunnel. It has not been established whether the differences between measured and calculated noise are due to facility differences, measurement techniques, or difficulty in modeling the aeroacoustic phenomena. This uncertainty may be resolved during planned flight tests of the propellers used in the study described in reference 10.

Helicopters

Helicopter noise is more difficult to predict than propeller noise because of the complex aerodynamic environment in which the rotors operate. The noise field is highly dependent upon aircraft geometry and aerodynamic environment, and the dominant noise generating mechanism may change with flight condition or observer locations.

Helicopter noise prediction methodology has been under development for many years. In spite of significant advances (for example, ref. 11), there is still no generally accepted method which can accurately predict helicopter rotor noise. Efforts to develop better methods have been hampered by the proprietary nature of helicopter noise prediction methods and a reluctance to share noise data because of competitive pressure and pending noise regulations. The absence of a high-quality and complete data base for a wide range of helicopter configurations has had a negative impact on the development and general acceptance of noise prediction theory.

Acquisition of a data base has also been hampered by the general lack of ground facilities with capability for acoustic tests of helicopter models. The only facility specifically designed for helicopter noise research is the Army indoor hover facility at the Ames Research Center, which has proved to be a valuable research tool. A number of other facilities have been used for helicopter noise research including the Ames 40 x 80 wind tunnel, the Langley V/STOL tunnel, and several smaller wind tunnels. Although each of these facilities is limited to some degree by acoustic characteristics, model size, or forward speed capability, some useful results can be obtained if care is taken in the experiment design. This may entail measuring noise in the near field, signal averaging to minimize background noise effects, or testing one configuration relative to another. For a variety of reasons, it has proven difficult to obtain good, absolute level data in the wind tunnel. It is this absolute data which is required for verifying and developing better noise prediction methods.

Flight tests may prove to be the best source of high-quality noise data. Two efforts were recently initiated to assemble existing flight-test data and use it to assess the status of current noise prediction methods. The data being assembled consists of noise data and rotor-blade pressure measurements for two helicopter configurations, as well as a complete set of flight parameters, and will be prepared with complete documentation in a format suitable for computer processing. These measured data are currently being used to evaluate a new noise prediction method based on an extension of the computer program described in ref. 9 and linear acoustic theory of reference 11. In addition, calculated aerodynamic inputs are being used to determine the sensitivity of the predicted noise to the quality of the input data.

One of the configurations being studied is shown in figure 4. It is in the 15 000-kg gross-weight range and has a 22-m diameter, six-bladed rotor with a tip speed of about 216 m/s. Although the study is not complete, there have been a number of preliminary comparisons between the predicted and measured noise data. Figure 5 shows a comparison for a 49-m/s flyover at 152-m altitude. The comparison was made using calculated rotor airloads for an observer on the ground, 305 m ahead of the aircraft. The agreement between predicted and measured noise levels is encouraging for the limited number of harmonics shown. The agreement for greater observer distances is not as good. This is due, at least in part, to the fact that only spherical spreading effects are included in the current calculations. An additional concern is that the original measured data contained ground reflection effects which were removed with a relatively simple correction method. These effects will require further investigation.

PROPELLER NOISE/PERFORMANCE DEMONSTRATION

The propeller noise/performance program is a joint NASA/EPA program to demonstrate that propeller noise for general aviation aircraft can be reduced in an economically reasonable manner. The goal of this effort is to reduce light aircraft propeller noise by 5 dB(A) while maintaining or improving propeller performance. The effort consists of (1) optimization studies to assess the potential noise and performance benefits of various propeller parameters, (2) wind-tunnel tests to verify design concepts, and (3) flight tests to demonstrate the noise reduction technology. Parallel efforts are being conducted at the Massachusetts Institute of Technology and the Ohio State University.

The parameters which affect both noise and performance were analyzed to determine the tradeoffs required to optimize the propeller. The results of one such parameter variation are shown in figure 6. This figure shows the calculated effect of varying the position of the peak of the radial load distribution on both the propeller noise and efficiency. The significant point is that the noise level can be reduced several dB(A) without a significant effect on propeller efficiency. This change combined with several other parameter changes can result in a significant noise reduction with little or no performance penalty.

In order to test some of the concepts which were developed during the parametric studies, two 1/4-scale model propellers were tested in an anechoic wind tunnel (ref. 2). The baseline propeller was a model of a standard Cessna 172 propeller. A "quiet" propeller was also constructed which had a slightly smaller diameter and a wider blade chord. The noise reduction was achieved through a reduction in tip speed due to the smaller diameter and the movement of the load distribution inboard on the propeller blade.

These propellers were tested over a wide range of conditions on a propeller spinning rig with and without an afterbody to simulate an aircraft fuselage. Figure 7 shows the test configuration in the acoustic wind tunnel with a fuselage afterbody.

After demonstrating the noise reduction techniques in the wind tunnel, full-scale propellers were designed for flight tests. Figure 8 shows the standard and "quiet" propellers mounted on a Cessna 172 aircraft. The aircraft was flown over a ground microphone array at 305-m altitude to determine the noise reduction under FAA noise certification conditions. In addition, aircraft rate of climb was measured over a range of airspeeds to determine the relative performance of the two propellers. These noise and performance results are also shown in figure 8. The "quiet" propeller consistently produced a noise reduction of about 5 dB(A) while retaining climb performance characteristics comparable to the standard propeller.

PROPELLER NEAR-FIELD NOISE

Design of acoustic treatment for an aircraft sidewall requires knowledge of the exterior noise impinging on the sidewall and the interior noise level desired, as well as knowledge of the basic sidewall structure. Impinging noise has been defined for both low-speed and high-speed propellers and sample results are presented in figures 9 and 10.

Low-Speed Propeller

Impinging noise from a low-speed propeller is illustrated in figure 9. The measurements were made on the fuselage of a twin-engine, light aircraft. Noise was measured using an array of 10 flush-mounted microphones, seven of which were located in a horizontal line, and four of which were in a vertical line in the propeller plane. Minimum clearance between the sidewall and the propeller tip was about 0.05 of the propeller diameter. Tests were run at several rpm/power combinations in static conditions and for several forward speeds in taxi tests. Extensive results are presented in reference 12; sample results are shown at the right of the figure. The results indicate that the empirical prediction agrees with results for static tests and the analytical result agrees at low frequencies with measured data from taxi tests. The analytical results were obtained using the computer program of reference 9 with empirical corrections for the effects of the sidewall (ref. 12). The difference between static and taxi test results is due to the ingestion of turbulence that is generated by the propeller inflow interacting with the ground. The lower noise levels associated with the taxi condition were obtained with a forward speed of about 20 m/s or more. From this figure (in addition to figures 1 and 2), it can be concluded that prediction procedures are adequate for noise levels of low-speed, general aviation propellers.

High-Speed Propeller

Near-field noise of a high-speed, propfan propeller is illustrated in figure 10. Test data in this figure were obtained from reference 13. The test setup is indicated in the sketch at the upper left of the figure. The propeller tested (shown in figure 3) was a 0.61-m-diameter model of a swept-blade propeller designed to operate at a forward speed of Mach = 0.8 at an altitude of 10.67 km. The blade sweep is designed to reduce noise and maintain aerodynamic performance. The tests were carried out in an anechoic chamber of an acoustic wind tunnel having airflow capability at Mach = 0.3. At the power conditions of the tests, the propeller was fully immersed in the airflow. To compensate for the lower speed of the airflow, the model propeller was run at increased rpm so the helical tip speed was the same on the model as the full-scale design condition. A boilerplate cylinder was located at 0.8 propeller diameter clearance from the model propeller to simulate the aircraft fuselage, and the impinging noise was measured with an array of microphones flush-mounted in the cylinder.

Contours of equal sound pressure level at the blade-passage frequency from this test are shown at the lower left and predicted contours (ref. 13) are shown at the lower center of the figure. Comparing measured contours with predicted contours shows that the highest level and its location ahead of the propeller plane are in agreement. While the overall appearance of the contours shows reasonable agreement, there are differences in the detailed shapes. Improvements in the prediction procedures discussed earlier may improve agreement. The same analytical procedure used to calculate the model results was also used to predict impinging noise for full-scale flight conditions and the results are shown at the lower right. For this flight condition, the maximum noise occurs aft of the propeller plane. The figure indicates that the highest level is 150 dB with a large area subjected to 148 dB.

THEORETICAL METHODS FOR INTERIOR NOISE REDUCTION

Light Aircraft

Theoretical methods for predicting interior noise levels in light aircraft are under development (ref. 14). The methods are intended for use in designing minimum-weight sidewall structures having sufficient noise transmission loss to provide passenger comfort. A number of mathematical models of the sidewall structure are being investigated to find the simplest model that provides accurate results. Figure 11 shows three sidewall models that are under investigation. When using the flexible panel/rigid stiffener model or the flexible panel/flexible stiffener model, an array of subpanels is assembled to represent the complete sidewall area.

The graph indicates the sensitivity of interior noise to added weight for three candidate noise control approaches. The noise measured used is A-weighted dB to represent passenger comfort; these results were obtained using the panel/rigid stiffener model. All three treatments consist of modifications of the skin properties. Each treatment is applied separately to the structure. The figure indicates that the curves for a given treatment tend to flatten out as weight increases, suggesting a "diminishing returns" type of behavior. Comparing the treatments shows that the damping provides the most interior noise reduction for a given weight and that increasing skin thickness provides comparatively small reductions. The reductions obtained by damping are substantial; the original level of 104 dB(A) is uncomfortable while the level of about 85 dB(A) is reasonably comfortable. The weight required (about 36 kg) is larger than desired but small compared to the aircraft weight/ payload.

The theoretical predictions have been verified using simple laboratory panel/box tests (ref. 15). The models are being extended by inclusion of acoustic treatments such as fiberglass wool and double walls, and the improved model is to be used in an investigation of optimum treatment for a twin-engine, light aircraft.

High-Speed Turboprop Aircraft

Theoretical studies have been carried out to determine the weight and configuration of fuselage sidewall acoustic treatment required to provide an 80-dB(A), cabin noise level in propfan-powered aircraft (refs. 16 and 17). Figure 12 summarizes the results. The study required the development of new, comprehensive interior noise prediction methods and considered wide-body, narrow-body, and executive aircraft flying at Mach = 0.8 at 9.14-km altitude. The fuselage sidewall structure consisted of skin, stringers, and rings and had dimensions and materials typical of current operational aircraft. The studies indicated that additional acoustic treatment weight is required in comparison with the treatment normally expected for turbofan powered versions of the study aircraft. Added treatment is required along the fuselage from a station slightly ahead of the forward propeller plane to the tail section and circumferentially around the fuselage above the passenger floor. The sidewall consists of the elements indicated in the sketch; however, the primary noise control action is provided by the masses of the inner trim panel and outer skin acting as a double-wall noise barrier. The weights required to provide the 80-dB(A) interior noise level are shown at the right. In general, these weights are less than 2.5 percent of gross weight. The shaded portion of the bar indicates the range of results obtained from variations of sidewall configuration and analysis methods. The weight penalty for the wide-body aircraft from these studies is slightly less than the weight obtained from the RECAT (reduced energy for commercial transportation) system study; thus, the previous result (RECAT) is confirmed by the more extensive and in-depth recent studies. The RECAT study showed that propfan-powered aircraft have a fuel-saving and direct-operating-cost advantage over turbofan aircraft, even after taking the acoustic weight penalty into account.

PASSENGER COMFORT

Comfort Prediction Model

A program at Langley Research Center has led to the development of a model for predicting passenger discomfort (or acceptance) for existing or future transportation vehicles. Input to the model, figure 13, is the passenger vibration and noise environment for the vehicle and output of the model is the total discomfort measured along a discomfort scale. Development of the model has involved: (1) empirical estimation of discomfort due to sinusoidal and/or random vibrations within single axes; (2) empirical estimation of the discomfort due to vibration in combined axes; and (3) application of empirically determined corrections for the effects of interior noise and duration of vibration. The discomfort scale used to measure the output of the model is displayed in figure 14. The scale is ratio in nature and anchored at discomfort threshold. The figure shows the relationship between the discomfort scale (ordinate of figure 14) and the corresponding percentage (abscissa of figure 14) of passengers who would rate that discomfort level as being uncomfortable. A value of unity along the discomfort scale corresponds to discomfort threshold, i.e., 50 percent of the passengers would be uncomfortable. Details of the methods and procedures used to derive this discomfort scale are given in references 18 and

19. A complete description of the relationship between vibratory inputs and discomfort can be obtained from references 20 and 21. The extensive information contained in these references has been incorporated in a computer program for ease of calculation. For purposes of illustration, figure 15 provides a comparison of various vehicles along the discomfort scale. The figure presents the discomfort level produced by various air and surface transportation vehicles, relative to discomfort threshold. The discomfort values for each vehicle were obtained by using actual measured vibration/noise levels as input to the ride comfort model. These results provide an estimate of absolute discomfort as well as a quantitative comparison (and ranking) between vehicles. For example, the commercial jet transport together with the Bay Area Rapid Transit system and a full-sized automobile provided the best ride quality, i.e., the discomfort levels of each are below discomfort threshold. The various rail vehicles (including the German Bundesbahn and magnetically levitated vehicle) produced estimates of passenger discomfort that were generally somewhat above discomfort threshold and discomfort was seen to increase as vehicle speed increased. A typical city bus produces a relatively large value of discomfort, although the most uncomfortable ride for which data are available was estimated for a helicopter interior noise and vibration environment. However, removal of the noise component of the helicopter ride environment resulted in a discomfort level estimate slightly below discomfort threshold, thus indicating that noise was the predominant source of passenger dissatisfaction within the helicopter. The absolute levels of discomfort and relative ranking of vehicles shown in the figure are in good agreement with actual passenger experience and, hence, provide face validity of the NASA ride comfort scale. Further, since the scale was developed as common to all types and combinations of vibration and noise, it provides a simple and concise index for comparing the individual/combined axis components of discomfort, as well as a design tool for estimating the tradeoffs to passenger ride quality of various noise/vibration vehicle inputs.

Combined Noise and Vibration

An important portion of this program has been directed at including in the model the effects of combined noise and vibration on passenger comfort. Figure 16 displays typical results of this research. The individual curves of figure 16 indicate the D-weighted noise level, dB, and vibration acceleration, g_{rms}, required to produce constant amounts of overall discomfort for combinations of noise and vibration. (See ref. 22 for additional information about development of the curves.) The solid curves of the figure represent subjective data for the range of physical factors investigated in these studies; whereas, the dashed curves represent extrapolations over an extended range of the physical factors. Although the extrapolations are felt to be reasonable, caution should be exercised in the use of the extrapolated values. The validity of the extrapolations remains to be verified by future research. As shown in figure 16, constant discomfort curves were generated for discomfort (DISC) values ranging from discomfort threshold (DISC = 1) to values as high as DISC = 6, corresponding to a very high degree of discomfort. The usefulness of figure 16 lies in the fact that it represents a very important source of information for determining the tradeoffs available between noise and vibration in terms of passenger discomfort. For example, at high levels of discomfort (e.g., DISC 5 or 6), variations of acceleration over the range shown result in small changes of discomfort level, indicating that noise level is the dominant factor in the determination of overall discomfort. For low levels of discomfort, however, the noise levels must be reduced substantially with increases of acceleration in order to maintain a constant degree of discomfort. This indicates that at the lower degrees of discomfort, both noise and vibration, contribute significantly to overall discomfort. Finally, it should be noted that the threshold of noise discomfort for the combined environment is approximately 75 to 78 dB, L_D.

Passenger Response to Tones

Recent fuel conservation measures have led to proposals for development of propeller-driven aircraft for use in commuter as well as high-speed, long-haul applications. The increased fuel efficiency of these vehicles could be offset, however, if passenger acceptance necessitates increased aircraft weight for purposes of noise reduction. A noise characteristic typical of such propeller-driven aircraft environments that may be critical to passenger comfort is the low-frequency tonal content. Research within the NASA Langley program to this point had not accounted for the effects of such noise on passengers. Consequently, an exploratory study was conducted to examine subjective response to propeller-type tone noises in combination with broadband (boundary layer) noise. The study was conducted in the Passenger Ride Quality Apparatus (PRQA) at Langley Research Center (ref. 23), shown in figure 17. The study involved a total of 96 subjects who evaluated synthesized noises using a 9-point discomfort category scale. The noises consisted of turbulent boundary layer noise combined with propeller-type noises in a factorial combination of blade-passage frequencies (50, 80, 100, 125, and 200 Hz), harmonic rolloff rates (0 and 10 dB/harmonic), tone/noise ratios (0, 10, and 20 dB), and noise levels (85, 90, 95, and 100 dB). The results of these tests indicated that noise level and blade-passage frequency (tones) were the primary noise characteristics that determine passenger reaction. The study results are summarized in figure 18, which displays mean subject ratings of discomfort as a function of A-weighted noise level. Mean subject rating was obtained by averaging the ratings of the 96 subjects for each noise. The mean subject ratings for the sounds with tones fell in the region between the dashed lines. For comparison, the subjects rated a sound containing no tones; the mean ratings for this sound are indicated by the solid line labeled "boundary layer noise" in the figure. There is a complex relationship between discomfort and various tonal characteristics (tone/noise ratio, fundamental frequency, and rolloff rate). Figure 18 indicates that the discomfort ratings of tonal noises range from slightly less than boundary layer (the lower dashed line), to more discomfort than boundary layer (the upper dashed line). The maximum difference between tonal noises and boundary layer noise can be quantified by comparing the upper dashed line with the solid line on the basis of equal subject rating, as indicated by the horizontal line at a rating of four. The data on this horizontal line indicate that the most uncomfortable tonal noise and the boundary layer noise are rated equal in discomfort when the tonal noise is

5 dB(A) lower in level than the boundary layer noise. Thus, to provide comfort in a propeller aircraft that is equal to the comfort in a turbofan aircraft, the noise level may need to be as much as 5 dB(A) less in the propeller aircraft, depending on the specific values of parameters such as tone/noise ratio, tone rolloff rate, and frequency of the fundamental tone. Currently, research is being planned to further examine subjective response and to develop a noise metric correction to account for the interior noise environments of this type of vehicle.

CONCLUDING REMARKS

This paper describes recent results of NASA and NASA-sponsored research on the prediction and control of noise from aircraft propellers and rotors. Control approaches considered include reduction of the noise generated by the propeller and reduction of the noise transmitted through the aircraft sidewall to the interior. Applications to general aviation aircraft, high-speed turboprop transports, and helicopters are reviewed, and an exploratory laboratory study of passenger response to propeller-like tonal noises is described.

Comparisons of predicted and measured noise from low-speed general aviation propellers indicate that the noise can be predicted with satisfactory accuracy provided sufficient effort is devoted to definition of detailed aerodynamic pressure distributions. Current prediction methods were used along with wind-tunnel model studies to develop a quiet propeller that was shown by flight test to reduce flyover noise by about 5 dB(A) in comparison with the standard propeller. Prediction of noise from high-speed propellers and helicopter rotors is more difficult because of the complex blade shape and aerodynamic flow field. However, fair agreement is obtained in the lower frequency harmonics, and several features of the noise generating mechanisms are under investigation to improve predictions. Theoretical studies have been carried out to design sidewall acoustic treatments for general aviation and high-speed turboprop aircraft. These studies indicate that sidewalls can be designed to provide acceptable cabin noise levels, but that additional weight is required. Passenger subjective ratings of tonal noises and comparison with ratings of broadband (boundary layer) noise indicated that tonal noise ratings range from slightly less uncomfortable to more uncomfortable than broadband, depending on the particular values of tone/noise ratio, tone fundamental frequency, and tone rolloff rate.

REFERENCES

1. Magliozzi, B.: The Influence of Forward Flight on Propeller Noise. NASA CR-145105, Feb. 1977.

2. Succi, George P.; Munro, David H.; and Zimmer, Jeffrey A.: Experimental Verification of Propeller Noise Prediction. AIAA Paper 80-0994, June 1980.

3. Farassat, F.; and Succi, George P.: A Review of Propeller Discrete Frequency Noise Prediction Technology with Emphasis on Two Current Methods for Time Domain Calculations. J. Sound and Vibration, vol. 71, no. 3, Aug. 1980.

4. Hanson, D. B.; and Fink, M. R.: The Importance of Quadrupole Sources in Prediction of Transonic Tip Speed Propeller Noise. J. Sound and Vibration, vol. 62, no. 1, Jan. 1979.

5. Boxwell, D. A.; Yu, Y. H.; and Schmitz, F. H.: Hovering Impulsive Noise - Some Measured and Calculated Results. NASA CP-2052, Part I, May 22-24, 1978.

6. Isom, M. P.: The Theory of Sound Radiated by a Hovering Transonic Helicopter Blade. Polytechnic Institute of New York Report, Poly-AE/AM No. 75-5, 1975.

7. Farassat, F.: Extension of Isom's Thickness Noise Formula to the Near Field. Letter to Editor, J. Sound and Vibration, vol. 67, no. 2, 1979.

8. Brooks, B. M.; and Metzger, F. B.: Acoustic Test and Analysis of Three Advanced Turboprop Models. NASA CR-159667, Jan. 1980.

9. Nystrom, P. A.; and Farassat, F.: A Numerical Technique for Calculation of the Noise of High Speed Propellers with Advanced Blade Geometry. NASA TP-1662, 1980.

10. Dittmar, James H.: A Comparison Between an Existing Propeller Noise Theory and Wind Tunnel Data. NASA TM-81519, May 1980.

11. Farassat, F.: Theory of Noise Generation from Moving Bodies with an Application to Helicopter Rotors. NASA TR-451, 1975.

12. Mixson, J. S.; Barton, C. K.; Piersol, A. G.; and Wilby, J. F.: Characteristics of Propeller Noise on an Aircraft Fuselage Related to Interior Noise Transmission. AIAA Paper 79-0646, Mar. 12-14, 1979.

13. Magliozzi, B.; and Brooks, Bennett M.: Advanced Turboprop Airplane Interior Noise Reduction-Source Definition. NASA CR-159668, Oct. 1979.

14. Vaicaitis, R.: Noise Transmission into a Light Aircraft. AIAA 78-197R, J. of Aircraft, vol. 17, no. 2, Feb. 1980.

15. Vaicaitis, R.; and Slazak, M.: Noise Transmission Through Stiffened Panels. J. Sound and Vibration, vol. 70, no. 3, 1980.

16. Rennison, D. C.; Wilby, J. F.; Marsh, A. H.; and Wilby, E. G.: Interior Noise Control Prediction Study for High-Speed, Propeller-Driven Aircraft. NASA CR-159200, Sept. 1979.

17. Revell, J. D.; Balena, F. J.; and Koval, L. R.: Analytical Study of Interior Noise Control by Fuselage Design Techniques on High-Speed, Propeller-Driven Aircraft. NASA CR-159222, July 1978.

18. Dempsey, T. K.: A Model and Predictive Scale of Passenger Ride Discomfort. NASA TM X-72623, Dec. 1974.

19. Dempsey, T. K.; and Leatherwood, J. D.: Vibration Ride Comfort Criteria. Proceedings of the Sixth Congress of the International Ergonomics Association, July 1976.

20. Dempsey, T. K.; Leatherwood, J. D.; and Clevenson, S. A.: Single Axis Vibration Discomfort Criteria. NASA TP-1422, May 1979.

21. Leatherwood, Jack D.; Dempsey, Thomas K.; and Clevenson, Sherman A.: A Design Tool for Estimating Passenger Ride Discomfort Within Complex Ride Environments. Human Factors Jour., vol. 22, no. 3, 1980.

22. Dempsey, T. K.; Leatherwood, J. D.; and Clevenson, S. A.: Development of Noise and Vibration Ride Comfort Criteria. J. Acoustical Society of America, vol. 65, no. 1, Jan. 1979.

23. Clevenson, S. A.; and Leatherwood, J. D.: On the Development of Passenger Vibration Ride Acceptance Criteria. Shock and Vibration Bulletin, vol. 43, no. 3, June 1973.

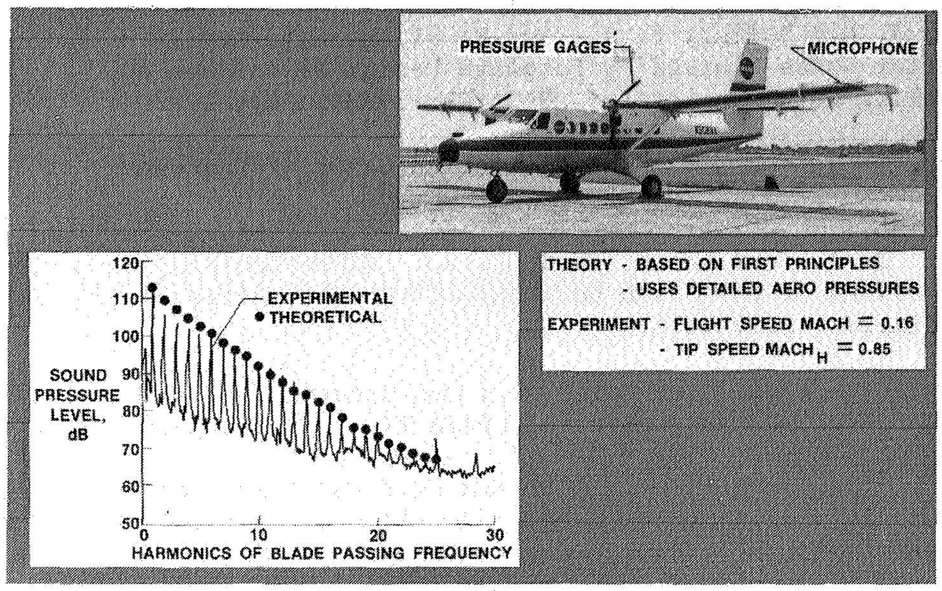

Figure 1.- Measured and predicted noise of general aviation propeller.

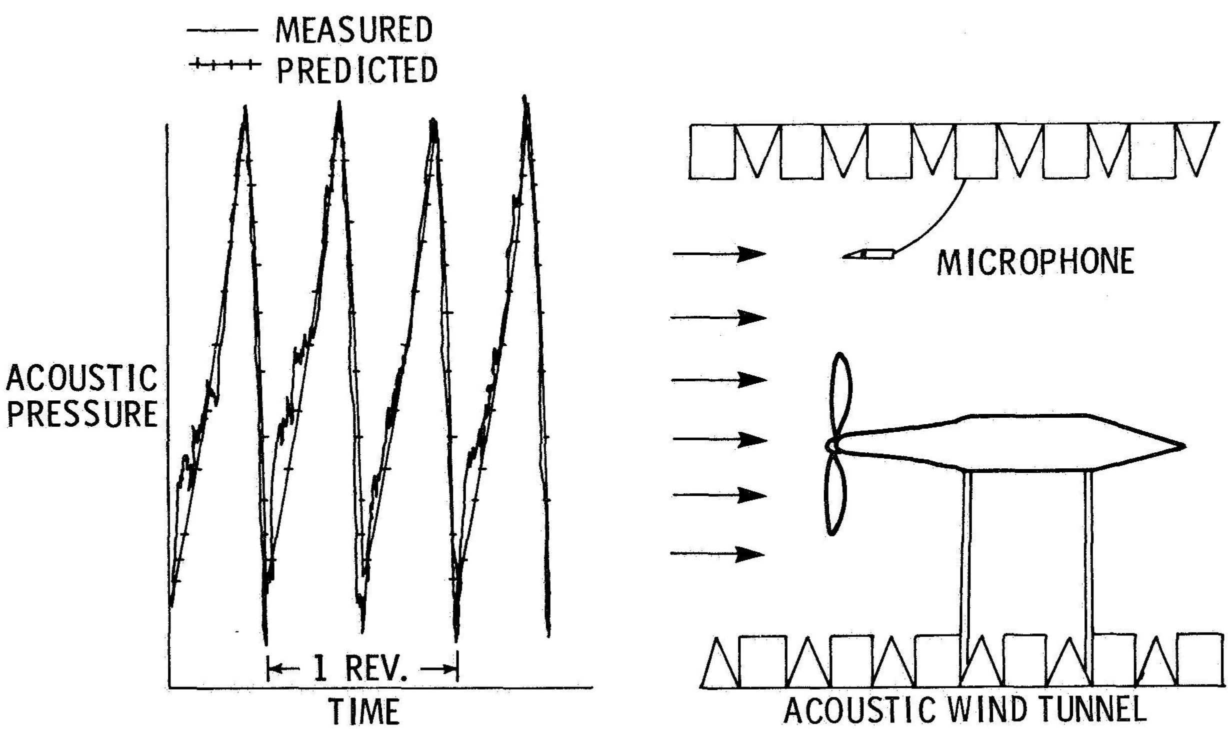

Figure 2.- Measured and predicted noise of general aviation propeller models.

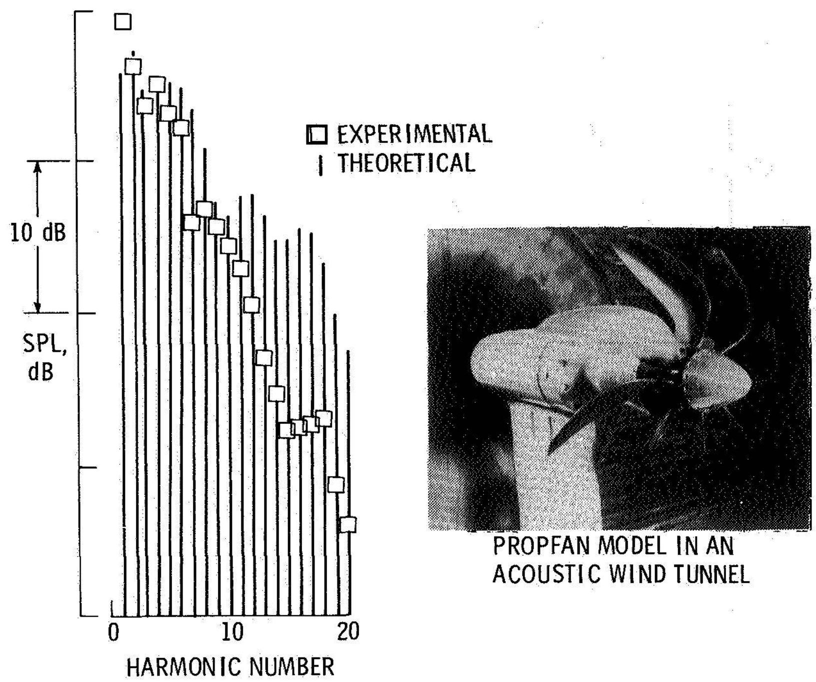

Figure 3.- Harmonic noise spectrum of model high-speed propeller. Diameter = 0.61 m.

Figure 4.- Large helicopter type used in flyover noise tests.

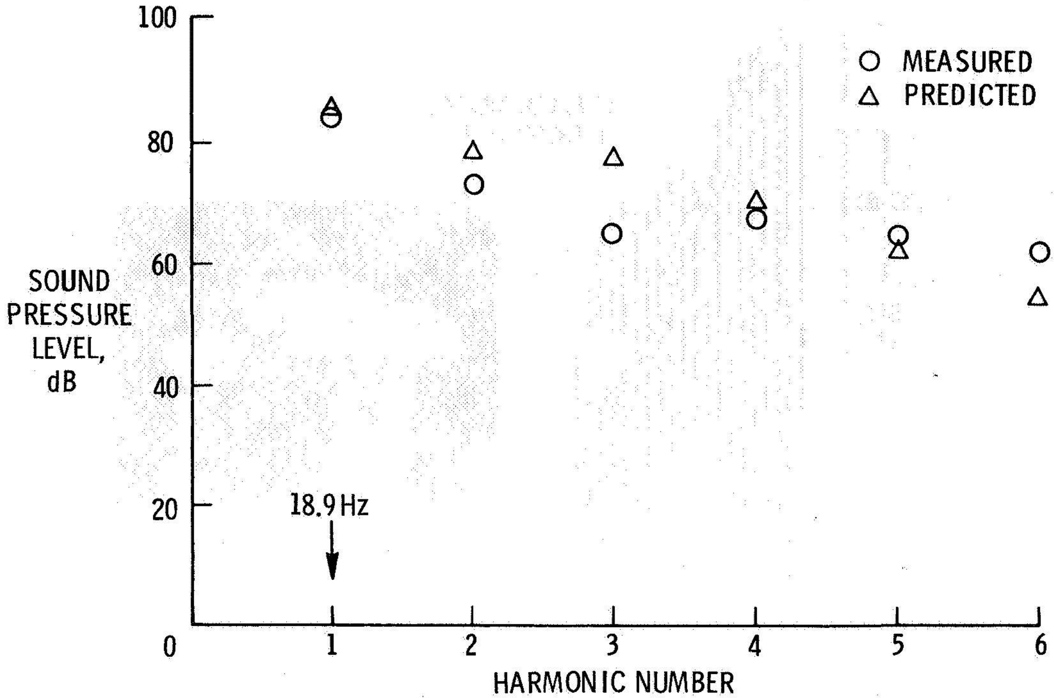

Figure 5.- Measured and predicted noise levels for helicopter in 49-m/s level flyover at 152-m altitude.

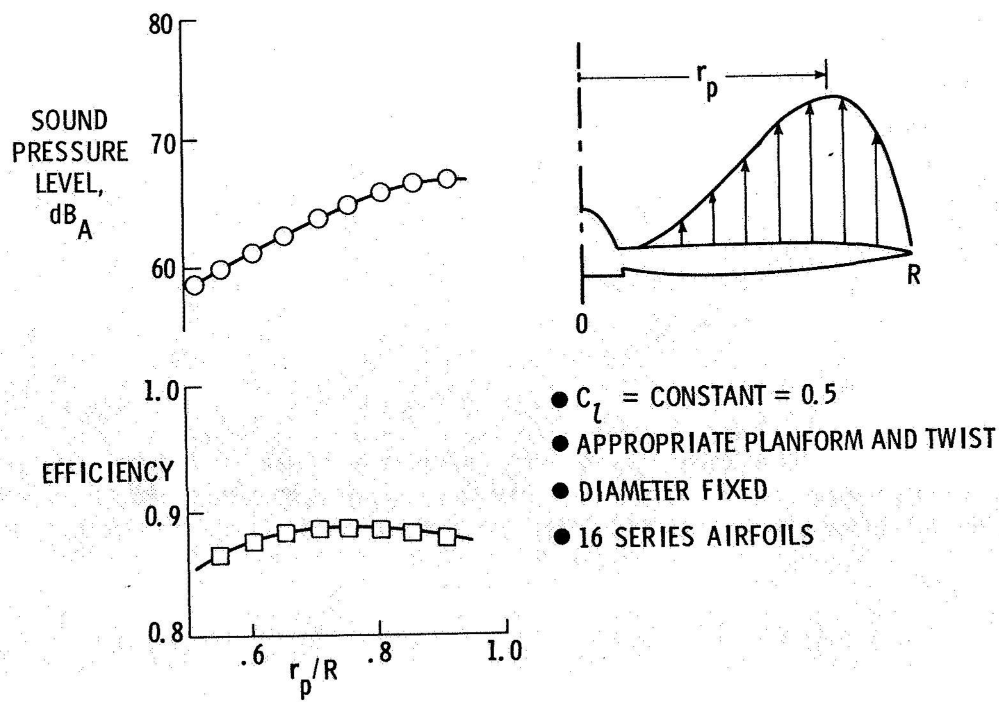

Figure 6.- Calculated effect of varying radial load distribution.

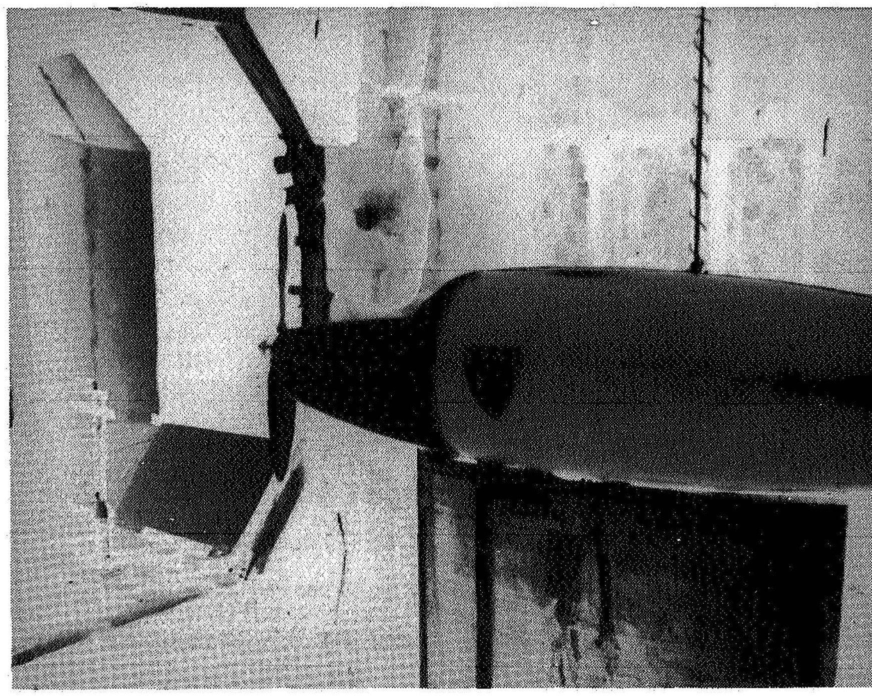

Figure 7.- Acoustic tests of quiet general aviation propellers in anechoic wind tunnel.

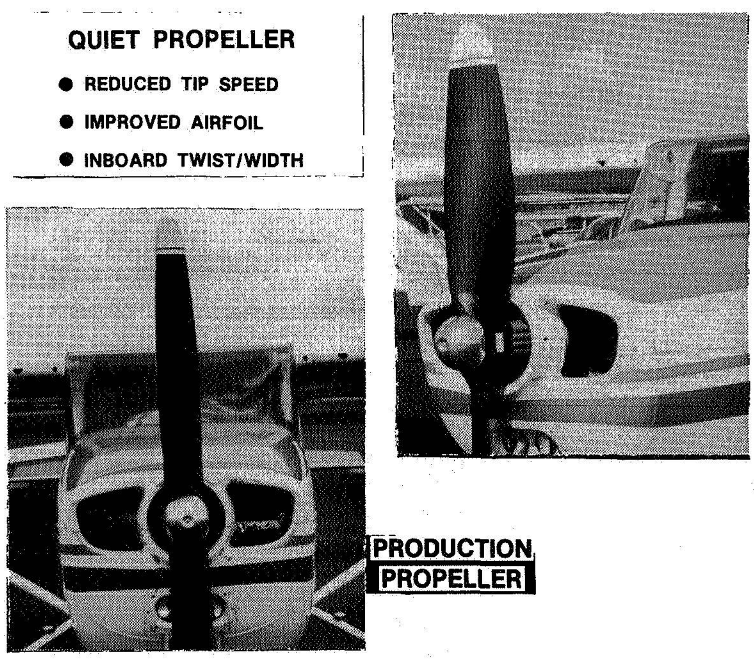

PROPELLER	FLYOVER NOISE
PRODUCTION	77.4 dBA
QUIET	72.6 dBA
GOAL: REDUCE BY 5 dBA	

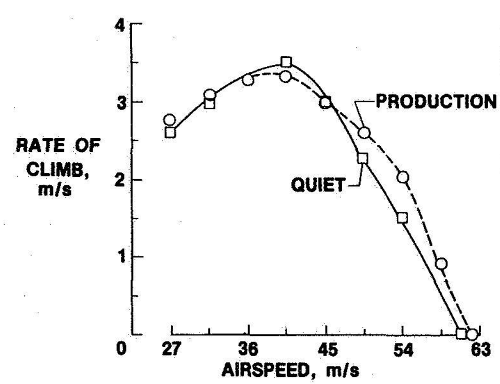

Figure 8.- Noise and performance flight demonstration.

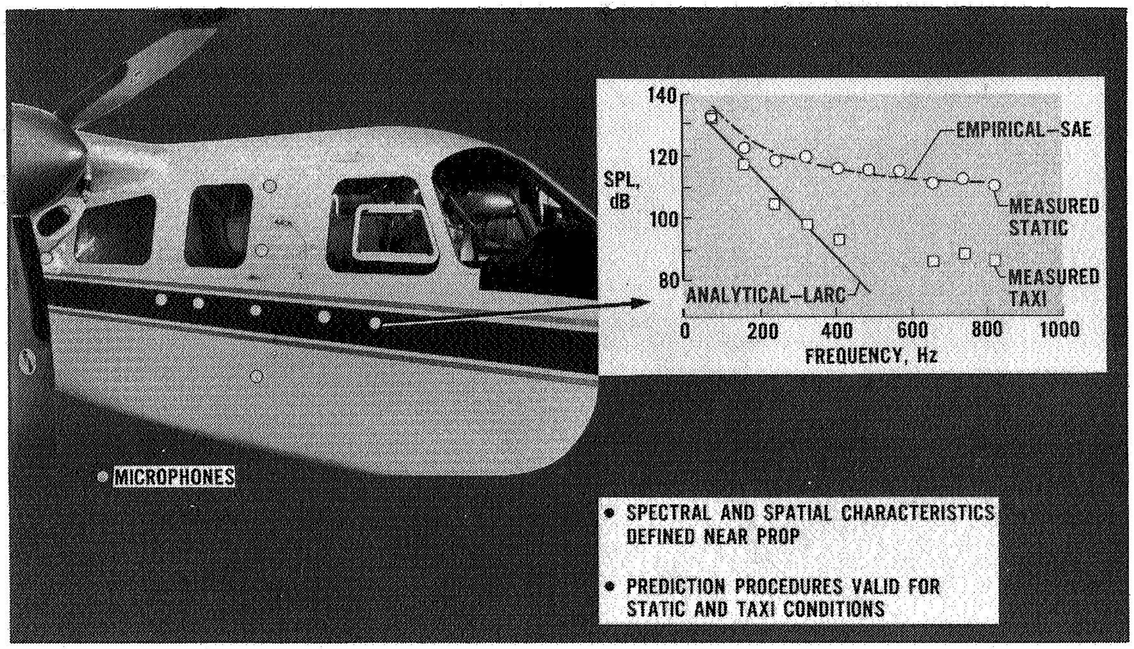

Figure 9.- Propeller noise on fuselage of twin-engine, light aircraft.

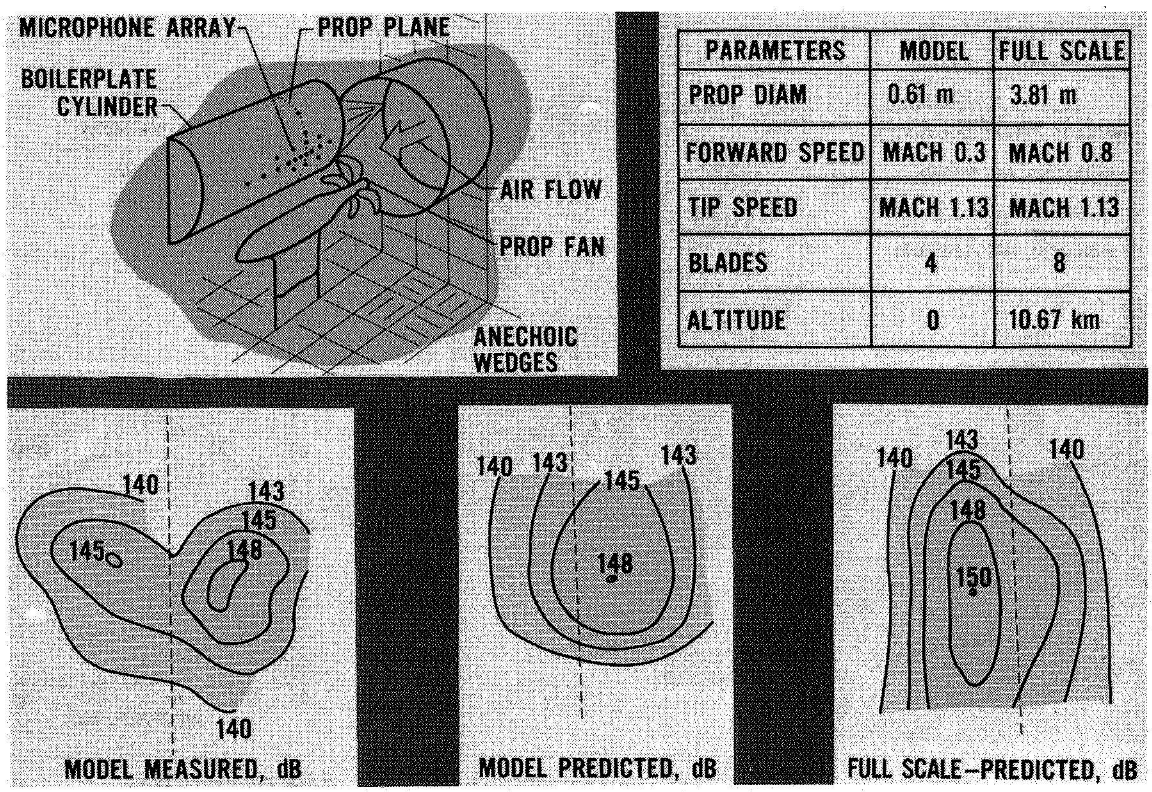

PARAMETERS	MODEL	FULL SCALE
PROP DIAM	0.61 m	3.81 m
FORWARD SPEED	MACH 0.3	MACH 0.8
TIP SPEED	MACH 1.13	MACH 1.13
BLADES	4	8
ALTITUDE	0	10.67 km

Figure 10.- Noise from model high-speed propeller on simulated fuselage.

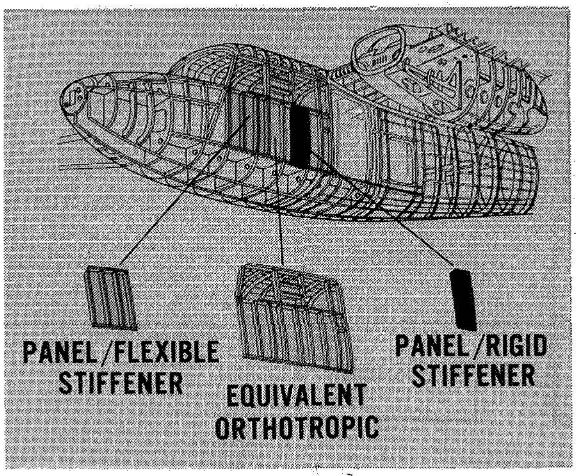

CHARACTERIZATION OF SIDEWALL

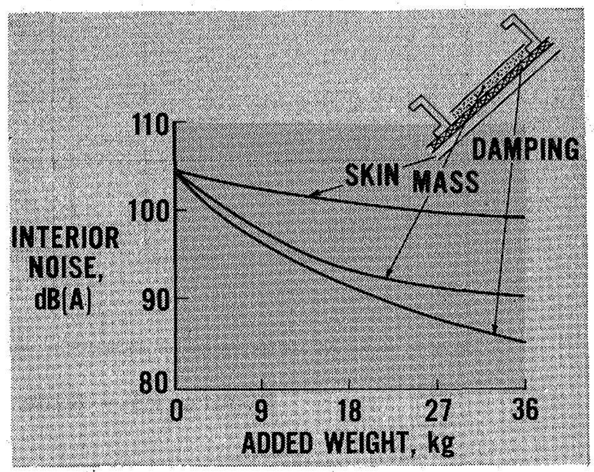

NOISE/WEIGHT SENSITIVITY STUDY

Figure 11.- Theoretical studies of interior noise control by sidewall treatment on light aircraft.

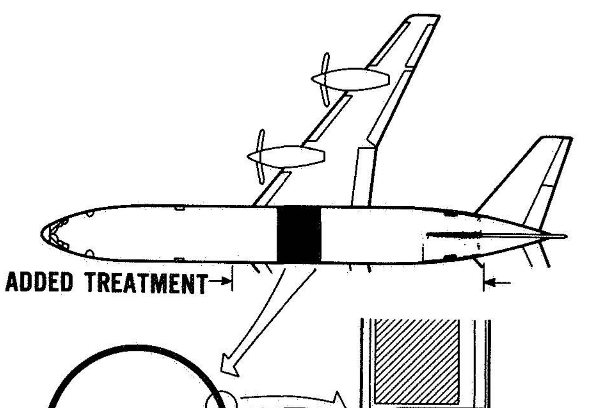

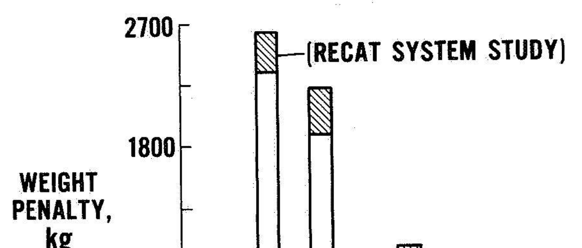

Figure 12.- Theoretical studies of sidewalls for interior noise control on high-speed turboprop aircraft.

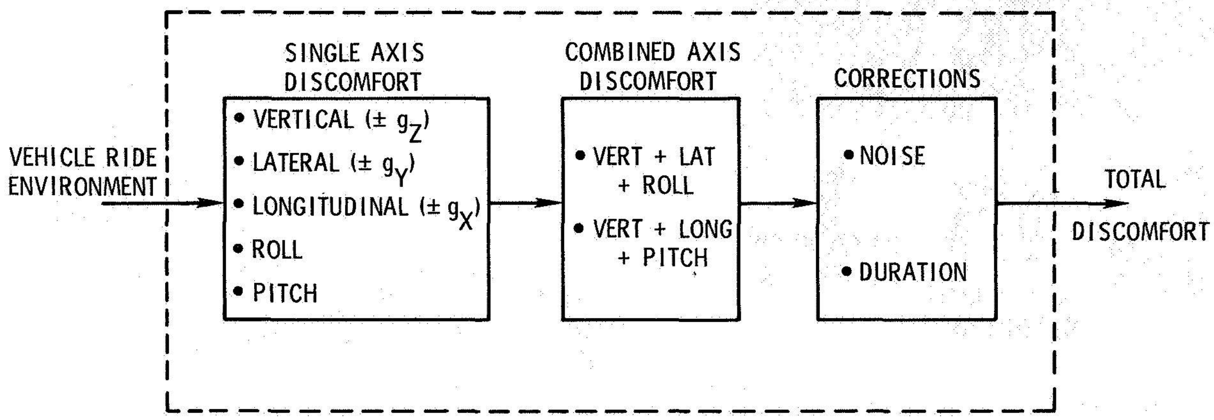

Figure 13.- Ride quality model.

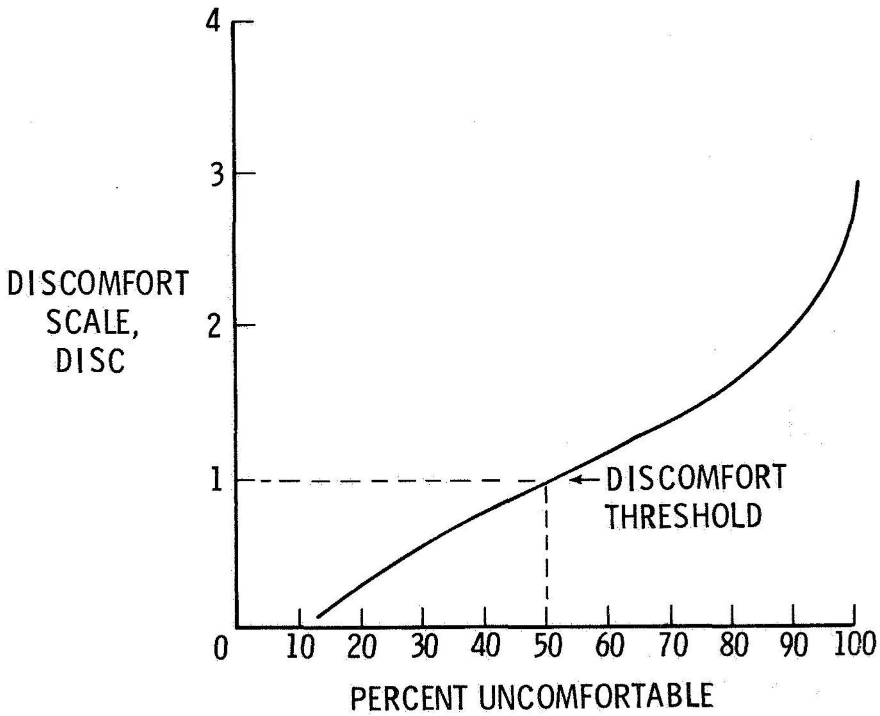

Figure 14.- Relation between discomfort scale and percent of passengers uncomfortable.

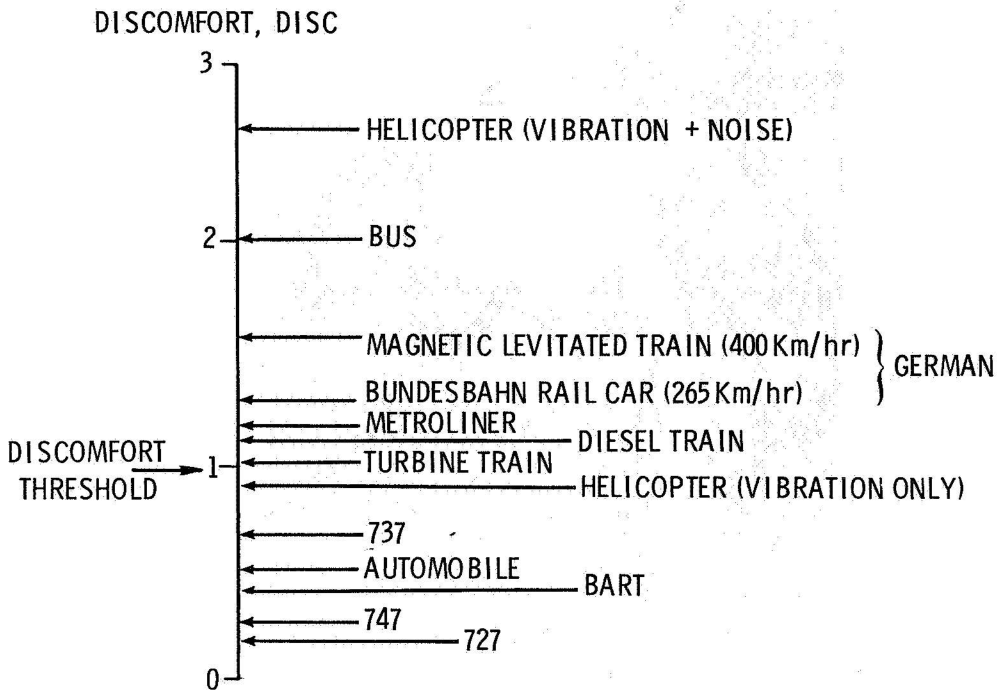

Figure 15.- Discomfort scale rating of transportation vehicles.

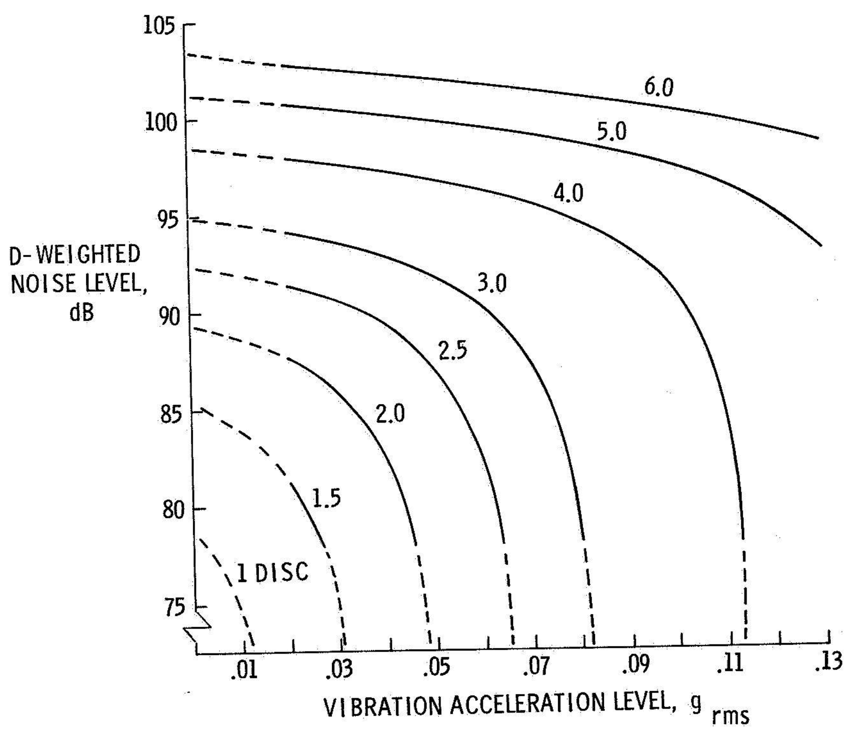

Figure 16.- D-weighted noise levels required to produce constant discomfort curves as function of vibration acceleration.

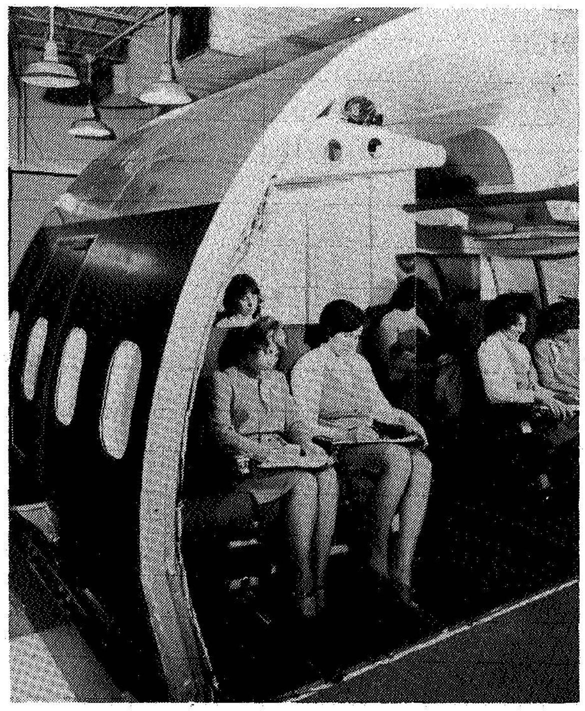

Figure 17.- The Passenger Ride Quality Apparatus at Langley Research Center.

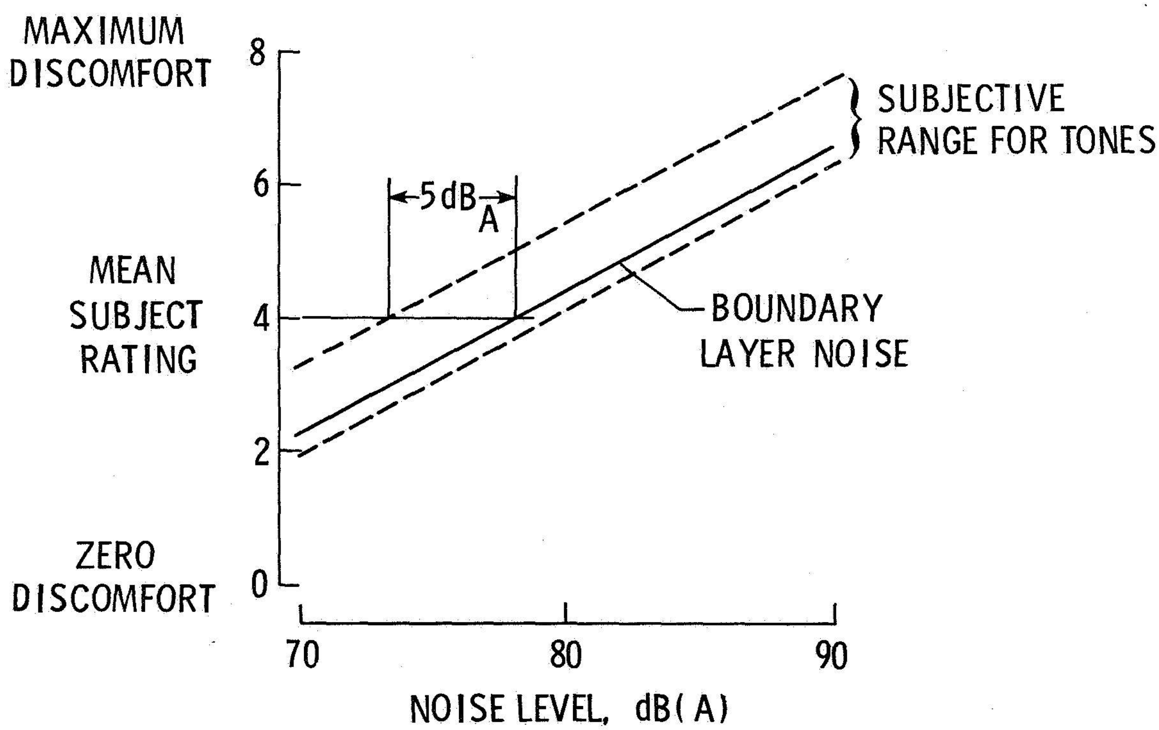

Figure 18.- Subjective response to tonal interior noise.